^{1}H NMR Evidence for a Left-Handed Helical Structure of Poly(ribocytidylic acid) in Neutral Solution

Michelle S. Broido*† and David R. Kearns*

Contribution from the Department of Chemistry, University of California, San Diego, La Jolla, California 92093. *Received September 21, 1981*

Abstract: A variety of one- and two-dimensional proton NMR relaxation techniques have been used to investigate the ordered structure of neutral poly(cytidylic acid) (poly(C)) in solution. These measurements indicate that there is an unexpectedly strong dipolar interaction between the H_5 proton of one cytidine residue with the $H_{1'}$ sugar proton of an adjacent nucleotide. This interaction is manifested in transient nuclear Overhauser effects, in a comparison of selective and semiselective relaxation rate measurements, and in two-dimensional Fourier transform spin-exchange experiments. A relatively strong interaction between the cytidine H_6 proton and $H_{1'}$ is also indicated. A theoretical model for treating internal motions in poly(C) has been developed and used to account for the observed relaxation rates. Satisfactory agreement is obtained by using an overall tumbling time for the poly(C) helix of 12 ns in conjunction with various internal motions with correlation times on the order of 1 ns and internuclear separations of $r(H_5-H_{1'}) = 2.3$ Å and $r(H_6-H_{1'}) = 2.4$ Å. A model incorporating these interproton distances has been constructed for the poly(C) helix and found to be left-handed. Two special features which may be responsible for stabilizing this unusual structure include direct hydrogen bonds between the carbonyl group of one base with the amino group of an adjacent residue and a direct hydrogen bond between the 2'-OH group and a phosphate oxygen in the backbone. This study represents the first application of 2D FT techniques to the investigation of polynucleotide structures in solution.

During the past 5 years there have been a number of nuclear magnetic resonance studies of the structural and dynamic properties of native and synthetic polynucleotides.[1-17] While relaxation methods have frequently been used in the ^{13}C and ^{31}P NMR experiments,[11-15] most of the ^{1}H studies have been restricted to measurement of spectra under different experimental conditions. Of the few proton relaxation measurements that have been carried out, most have concentrated on the determination of nonselective spin–lattice relaxation rates,[15-17] which are usually complicated by spin-diffusion effects[18-20] that are present, even in relatively low molecular weight DNA and RNA samples (e.g., M_r 8000).[21,22] However, by carrying out a combination of selective and semiselective T_1 measurements, ^{1}H relaxation data can be used to investigate both the structural and dynamic properties of polynucleotides in solution.[21,23,24] Considerable additional information about the dipolar (H–H) interactions can be obtained through the two-dimensional spin-exchange experiments recently introduced by Ernst and co-workers.[25-28]

In the present studies various ^{1}H relaxation techniques have been used to investigate the structural and dynamic properties of the single-stranded RNA polymer poly(ribocytidylic acid) (poly(C)) in neutral solution. Numerous previous studies indicate that this "simple" homopolymer has some sort of ordered helical structure at temperature below 30 °C, but there is little definitive evidence concerning the nature of this ordered state.

Ts'o et al. had suggested a typical random coil structure for poly(C) at pH 7.5,[29] because both the specific rotation and the molar extinction coefficient exhibit noncooperative melting behavior, but examination of similar optical data led Bloomfield et al.[2] to conclude that poly(C) in solution has stacked bases with a nonrigid structure "in which the bases undergo (constrained) torsional oscillation plus extension and compression". Circular dichroism[30] and ORD[31] studies on poly(C) at pH ~7 indicate a "highly asymmetric, probably helical structure" for poly(C).[31] Laser temperature jump studies by Freier et al. indicate that the lifetime of the ordered state in poly(C) is ~100 ns and that high NaCl concentrations tended to decrease the rate of disordering while formamide and acetonitrile increased the rate of disordering.[32] Chen and Charney[33] were unsuccessful in their attempt to orient single-stranded poly(C) in an electric field, but Causley and Johnson observed ordering of poly(C) in a flow birefringence experiment.[34]

Raman studies of poly(C) in neutral solution show spectral frequencies characteristic of a neutral cytosine ring and of an ordered phosphodiester group with A-type geometry of the C–O–P–O–C linkages.[35,36] However, frequencies assigned to ribose

† Present address: Department of Isotope Research, Weizmann Institute of Science, Rehovot, Israel.

(1) T. L. James, "Nuclear Magnetic Resonance in Biochemistry", Academic Press, New York, 1975.
(2) V. A. Bloomfield, D. M. Crothers, I. Tinoco, Jr., "Physical Chemistry of Nucleic acids", Harper and Row, New York, 1974.
(3) W. Guschlbauer, "Nucleic Acid Structure", Springer-Verlag, New York, 1976.
(4) G. Girjesh and I. C. P. Smith, *Biopolymers*, **12**, 2589 (1973).
(5) D. J. Patel, *Eur. J. Biochem.*, **83**, 452 (1978).
(6) D. J. Patel, *J. Polym. Sci., Polym. Symp.*, **62**, 117 (1978).
(7) D. R. Kearns, *Annu. Rev. Biophys. Bioeng.*, **6**, 477 (1977).
(8) T. A. Early and D. R. Kearns, *Proc. Natl. Acad. Sci. U.S.A.*, **76**, 4165 (1979).
(9) D. J. Patel and L. L. Canuel, *Eur. J. Biochem.*, **96**, 267 (1979).
(10) M. E. Hogan and O. Jardetzky, *Proc. Natl. Acad. Sci. U.S.A.*, **76**, 6341 (1979).
(11) K. Akasaka, A. Yamada, and H. Hatano, *FEBS Lett.*, **53**, 339 (1975).
(12) K. Akasaka, *Biopolymers*, **13**, 2273 (1974).
(13) P. H. Bolton and T. L. James, *J. Phys. Chem.*, **83**, 3359 (1979).
(14) P. H. Bolton and T. L. James, *Biochemistry*, **19**, 1388 (1980).
(15) F. Hayashi, K. Akasaka, and H. Hatano, *Biopolymers*, **16**, 655 (1977).
(16) F. Hayashi, S. Shibata, K. Akasaka, and H. Hatano, *J. Magn. Reson.*, **28**, 397 (1977).
(17) J. M. Neuman and S. Tran-Dinh, *Biopolymers*, **20**, 89 (1981).
(18) A. Kalk and H. J. C. Berendsen, *J. Magn. Reson.*, **24**, 343 (1976).
(19) A. A. Bothner-By in "Biological Applications of Magnetic Resonance", Academic Press, New York, 1979, p 177.
(20) W. E. Hull and B. D. Sykes, *J. Chem. Phys.*, **63**, 867 (1975).
(21) T. A. Early and D. R. Kearns, *Nucl. Acids Res.*, **8**, 5795 (1980).
(22) D. R. Kearns, N. Assa-Munt, R. W. Behling, T. A. Early, J. Feigon, J. Granot, W. Hillen, and R. D. Wells, in "Biomolecular Stereodynamics Vol. I", R. H. Sarma, Ed., Adenine Press, New York, 1981, pp 345–366.
(23) T. A. Early, D. R. Kearns, W. Hillen, and R. D. Wells, *Biochemistry*, **20**, 3764 (1981).
(24) T. A. Early, D. R. Kearns, W. Hillen, and R. D. Wells, *Biochemistry*, **20**, 3756 (1981).
(25) J. Jeener, B. H. Meier, P. Bachmann, and R. R. Ernst, *J. Chem. Phys.*, **71**, 4546 (1979).
(26) B. H. Meier and R. R. Ernst, *J. Am. Chem. Soc.*, **101**, 6441 (1979).
(27) S. Macura and R. R. Ernst, *Mol. Phys.*, **41**, 95 (1980).
(28) K. Nagayama, P. Bachmann, K. Wüthrich, and R. R. Ernst, *J. Magn. Reson.*, **31**, 133 (1978).
(29) P. O. P. Ts'o, G. K. Helmkamp, and C. Sander, *Biochim. Biophys. Acta*, **55**, 584 (1962).
(30) J. Brahms, *J. Am. Chem. Soc.*, **85**, 3298 (1967).
(31) G. D. Fasman, C. Lindblow, and L. Grossman, *Biochemistry*, **3**, 1015 (1964).

0002-7863/82/1504-5207$01.25/0

vibrations behaved in a way that suggested a conformation different from that usually found in ribopolymers (single or double stranded).[35,36]

These previous investigations suggest that poly(C) does have an ordered structure at neutral pH and at low temperature which is at least partially helical, but which differs from other ordered ribopolymers in some aspect of the sugar–phosphate backbone. In the present study, various ^1H nuclear magnetic resonance (NMR) spin–lattice relaxation measurements have been used to investigate the structure and dynamics of poly(C) in neutral solution. On the basis of these NMR results, we are able to propose a structure for the ordered form of neutral poly(C). The proposed structure not only accounts for the relaxation results but also accounts for the unusual stability of the amino and hydroxyl protons with regard to exchange with water protons.[37] A preliminary account of this work has been presented elsewhere.[38]

Experimental Section

Materials. Poly(cytidylic acid) of average molecular weight greater than one million (35 000+ nucleotides) (Sigma Chemical Co.) was subjected to lanthanide digestion, and the resulting small polymer fragments (5–200 nucleotides in length) were separated, collected, and sized by gel electrophoresis.[39,40] This procedure was devised and carried out by Dr. Deborah B. Lerner in this laboratory.

Samples of the sized poly(C) were prepared for ^1H NMR studies by vacuum dialysis against solutions containing 0.1 M NaCl, 0.02 M K_3PO_4, 0.002 M EDTA, pH 7.1, in doubly distilled water. The final nucleic acid concentrations were approximately 15 mM in phosphate (concentrations determined spectrophotometrically, assuming ϵ_{260} 5200 L/(mol cm)). Aliquots of sample were repeatedly dried with a Buchler Instruments Evapomix and then redissolved in 99.8% D_2O (Wilmad) a minimum of 3 times. The final aliquot of D_2O used had an isotopic purity of 99.998% (Merck).

EDTA was used to complex any paramagnetic ions which, if present in the solution, would have profound effects on measured relaxation times. That the EDTA did not affect the relaxation behavior of the poly(cytidylic acid) protons was confirmed by comparison of experiments run with and without EDTA, by comparison of relaxation experiments in which the EDTA resonances were or were not saturated, and by the absence of any cross-peaks between the EDTA resonances and any of the poly(C) resonances in the 2D exchange experiments.

Several preliminary experiments were performed to determine optimum sample conditions. A sample was degassed to remove any possible effects of dissolved paramagnetic oxygen; relaxation rates were no different than those of an undegassed sample. With sample run in "wet" D_2O (lower isotopic purity, higher H_2O content) the HOD peak began to dominate the spectra, but the relaxation rates were not affected. A 5 mM sample was prepared and examined in order to evaluate the effect of intermolecular interactions on relaxation rates. Comparison of resulting relaxation rates with those of a 25 mM sample showed no differences. In most cases we therefore used samples in the 10–15 mM range.

Methods. NMR measurements were performed either at 220 MHz on a Varian HR-220 or at 300 MHz on a Varian HR-300 spectrometer modified to operate as an FT spectrometer by Dr. Thomas Early. Temperatures on both the HR-220 and HR-300 were determined with commercially standardized samples of ethylene glycol. At 300 MHz, 20 ± 4 scans were needed for adequate signal-to-noise ratios, whereas at 220 MHz, 100–200 scans were required.

Nonselective spin–lattice relaxation experiments were performed on both the HR-220 and the HR-300 by the standard inversion–recovery pulse sequence $[180°-\tau-90°-\text{acquisition}-D_5-]_n$, where D_5 is a fixed delay time during which equilibrium magnetization is reestablished.[41] Although it is usual to let τ vary over a range $(0–1.5)T_1$, this was not feasible for the poly(C) studies because of the multicomponent nature of the relaxations. Therefore, to stay within the "initial rate approximations", τ was varied within $(0–0.3)T_1$. D_5 was typically 7–10 times the T_1 of the slowest relaxing proton in the poly(C) system; 180° pulses were typically 100 μs on the HR-220 and 165 μs on the HR-300.

Nonselective spin–lattice relaxation experiments were also performed with one of the resonances in the spectrum being continuously irradiated and saturated. The large negative nuclear Overhauser effects (NOE) in poly(cytidylic acid) led to very low intensity of the nonirradiated peaks and, consequently, poor signal-to-noise. Also, the extent of saturation differed from experiment to experiment; hence, results from these experiments, while qualitatively useful, are of limited quantitative value.

Selective spin–lattice relaxation measurements were performed by application of a weak (20–40 ms) pulse at the center of a given resonance. Such pulses typically excited spins at frequencies ±30 Hz from the pulse rf frequency. The pulse sequence was $[180°(\text{selective})-\tau-90°(\text{nonselective})-D_5-]_n$.

Two-dimensional spectra were obtained with the sequence $90°_x-t_1-90°_x-t_M-90°_x$ (acquisition, t_2),[26-28] where t_1 was incremented by 500 μs, and t_M, the mixing time, was held constant. During the mixing period a homospoil pulse, typically 20 ms, was applied. After each pulse sequence there was a delay of about 20 s to allow return of the magnetization to equilibrium. A typical experiment required approximately 20 h.

A Kendrew wire model, generously provided by Dr. Joseph Kraut, was used to construct a model of poly(C).

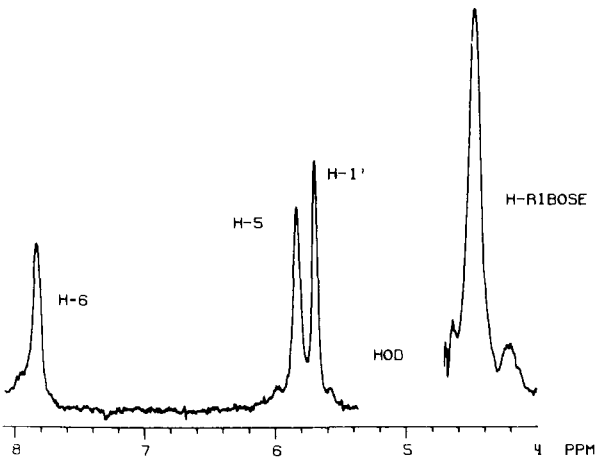

Figure 1. 300-MHz spectrum of poly(cytidylic acid) (70mer) at 23 °C.

Table I. Effect of Spectrometer Frequency on the Nonselective Spin-Lattice Relaxation Rates (s^{-1}) of 70mer Poly(C)

resonance	R^0_1 (220 MHz, 22 °C)	R^0_1 (300 MHz, 23 °C)	$\frac{R^0_1\ (220)}{R^0_1\ (300)}$
H_6	1.05 ± 0.04	0.65 ± 0.03	1.62
H_5	0.83 ± 0.04	0.54 ± 0.03	1.54
H_1'	0.69 ± 0.05	0.48 ± 0.02	1.48
H_{sugar}	1.04 ± 0.04	0.77 ± 0.03	1.35

Results

The normal one-dimensional ^1H spectrum of poly(C) at 23 °C in neutral aqueous solution contains three resolved lines of 20–40 Hz line width downfield of the HOD (H_2O) resonance and several poorly resolved resonances just upfield of the HOD (see Figure 1). The peaks at 7.84, 5.84, and 5.68 ppm (at 23 °C) are assigned to H_6, H_5, and $H_{1'}$, respectively. The four upfield resonances (~4.5 ppm) arise from nonexchangeable ribose protons, and a fifth ribose resonance is buried under the water signal. Between 20 and 70 °C there is little change in the chemical shifts of the various resonances (less than 0.2 ppm, with most changes less than 0.1 ppm).

One-Dimensional Relaxation Measurements. The most commonly performed spin–lattice relaxation experiment is the nonselective inversion–recovery sequence $[180°-\tau(\text{variable})-90°-\text{detect}]_n$ in which the initial 180° pulse inverts all spins in the system and the subsequent return to thermal equilibrium is then monitored after application of a nonselective 90° pulse. It is also

(32) S. M. Freier, K. O. Hill, T. G. Dewey, L. A. Marky, K. J. Breslauer, and D. H. Turner, *Biochemistry*, **20**, 1419 (1981).
(33) H. H. Chen and E. Charney, *Biopolymers*, **19**, 2123 (1980).
(34) G. C. Causely and W. C. Johnson, Jr., *Biophys. J.*, **33**, 321a (1981).
(35) B. Prescott, R. Gamache, J. Livramento, and G. J. Thomas, Jr., *Biopolymers*, **13**, 1821 (1974).
(36) C. H. Chou and G. J. Thomas, Jr., *Biopolymers*, **16**, 765 (1977).
(37) P. H. Bolton and D. R. Kearns, *Biochim. Biophys. Acta*, **517**, 329 (1978).
(38) M. S. Broido and D. R. Kearns, *J. Magn. Reson.*, **41**, 496 (1980).
(39) D. B. Lerner and D. R. Kearns, *Biopolymers*, **20**, 803 (1981).
(40) D. B. Lerner and D. R. Kearns, unpublished results.
(41) E. D. Becker, "High Resolution NMR: Theory and Chemical Applications", 2nd ed., Academic Press, New York, 1980.

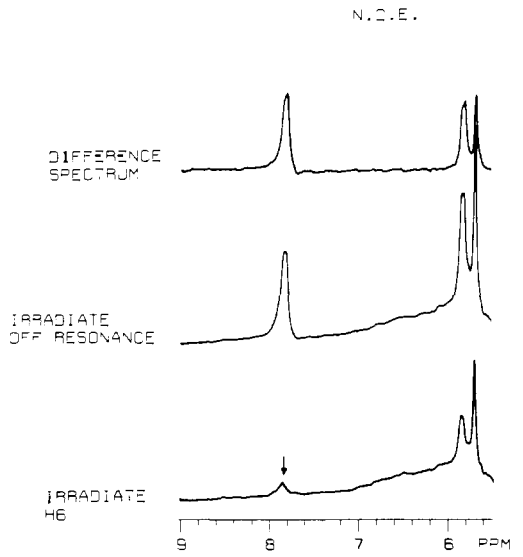

Figure 2. 220-MHz spectra of 70mer poly(C) at 22 °C showing effects of saturation of the H_6 resonance (indicated by arrow).

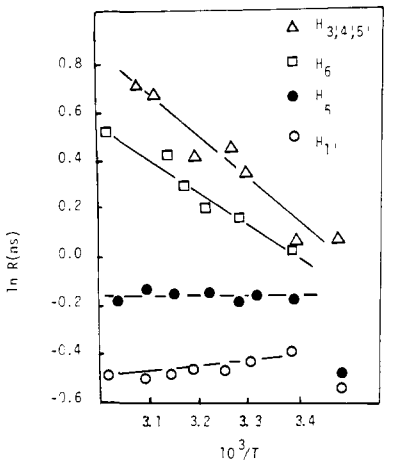

Figure 3. Plots of initial values of the nonselective spin–lattice relaxation rate vs. reciprocal temperature (220 MHz) for protons of poly(C) 70mer.

Table II. Effect of Polymer Size on the Nonselective Relaxation Rates (s^{-1}) of Poly(C) at 23 °C and 300 MHz

polymer size	resonance			
	H_6	H_5	$H_{1'}$	H_{sugar}
CpC	1.34	0.64	0.71	
17 ± 3	0.68 ± 0.03	0.48 ± 0.03	0.35 ± 0.03	0.89 ± 0.06
				0.83 ± 0.04
70 ± 10	0.65 ± 0.03	0.54 ± 0.03	0.48 ± 0.02	0.77 ± 0.02
95 ± 10	0.56 ± 0.03	0.60 ± 0.04	0.48 ± 0.02	0.75 ± 0.04

possible to invert a single (some small number of) resonance(s) with an initial selective (semiselective) 180° pulse and then use a nonselective 90° pulse to monitor the initial rate of return of the inverted spin(s) to thermal equilibrium, unperturbed by cross-relaxation with other spins. If there is significant cross-relaxation in the system, then the magnetizations of the noninverted resonances will also be affected after a sufficient period of time (see below).

Figure 2 shows an example of the large negative Overhauser effects and the spin diffusion resulting from selective saturation. These effects indicate significant cross-relaxations are occurring in the molecule.[18] Tables I and II summarize the effects of spectrometer frequency and polymer size on the room temperature nonselective spin–lattice relaxation rate (R^0(ns)), where the zero superscript denotes initial value of relaxation rates. The effect of temperature on R^0(ns) is summarized in Figure 3. For H_6 and the upfield sugar resonances, the nonselective relaxation rates

Table III. Relaxation Rates (s^{-1}) of Nonsaturated Resonances upon Selective Saturation of Resonance "xxx" in Poly(C) 70mer at 220 MHz, 23 °C

resonance saturated	H_6	H_5	$H_{1'}$	H_{sugar}
H_6	xxx	1.54 ± 0.20	1.32 ± 0.30	
H_5	1.97 ± 0.20	xxx	1.10 ± 0.18	1.46 ± 0.18
H_5, $H_{1'}$	2.64 ± 0.23	xxx	xxx	
$H_{1'}$	2.05 ± 0.20	1.53 ± 0.20	xxx	1.91 ± 0.24
H_{sugar}	3.48 ± 0.20	1.32 ± 0.18	1.72 ± 0.15	xxx

Table IV. Effect of Temperature on the Selective Spin–Lattice Relaxation Rates (s^{-1}) of Poly(C) 70mers at 220 MHz

resonance	temp, °C		
	22	28	40
H_6	8.28 ± 0.37	5.81 ± 0.35	3.19 ± 0.15
H_5	3.31 ± 0.19	2.21 ± 0.07	1.41 ± 0.12
$H_{1'}$	3.80 ± 0.12	2.31 ± 0.08	1.45 ± 0.15
H_{sugar}	4.11 ± 0.16		

Table V. Semiselective Relaxation Rates on Poly(C) 70mers at 220 MHz[a]

resonance	temp, °C		
	22	28	40
H_5	2.32 ± 0.12	2.12 ± 0.07	1.39 ± 0.06
$H_{1'}$	2.96 ± 0.17	2.35 ± 0.12	1.41 ± 0.08

[a] Both H_5 and $H_{1'}$ resonances inverted initially.

increase with increases in temperature whereas the nonselective relaxation rates of H_5 and $H_{1'}$ are relatively insensitive to temperature.

Table III lists the relaxation rates for the residual intensities of nonirradiated protons when a particular resonance in the system is subjected to a continuous, saturating field. Although these data are of qualitative value, their quantitative accuracy is suspect (see Methods).

The 220-MHz selective spin–lattice relaxation rates of the 70mer are given in Table IV. In the temperature range studied, all selective rates are larger than the corresponding nonselective rates, and in contrast to the nonselective rates, the selective rates decrease with increasing temperature. Semiselective relaxation rates resulting from simultaneous inversion of the H_5 and $H_{1'}$ resonances are given in Table V. These rates also decrease with increasing temperature, and by 40 °C, the selective and semiselective relaxation rates are identical.

The 180°(selective)–τ–90°(nonselective)–t_2 pulse sequence employed in the measurement of the selective relaxation rates (R^0(s)) allows for the concurrent determination of transient nuclear Overhauser effects.[42] If Overhauser effects are present, peaks will appear at frequencies other than that of the selective inversion in the difference spectra obtained by subtracting the $\tau \neq 0$ spectrum (for each individual value of τ) from that obtained when $\tau \simeq 0$, typically 5 ms. If such peaks have negative intensities, NOE's are positive, and vice versa. Figure 4 presents the 23 °C difference spectra resulting from selective inversion of H_6. From these spectra, it can be concluded that at 23 °C, there is a dipolar interaction between H_6 and both H_5 and $H_{1'}$ and with some of the upfield sugar protons. Similar measurements in which H_5 was selectively inverted indicate that H_5 and $H_{1'}$ interact with each other and with the upfield sugar protons.

Two-Dimensional Relaxation Measurements. A two-dimensional exchange experiment with the pulse sequence [90°$_x$–t_1–90°$_x$–τ_M–90°$_x$–t_2]$_n$ provides an efficient means of elucidating dipolar connectivities in a molecule. The experiment is repeated, with t_1 being stepped through in incremental values; Fourier transformation of both the t_1 and t_2 time variables leads to the 2D spectrum.[26] Peaks are located by the coordinates (ω_2,ω_1),

(42) S. L. Gordon and K. Wütrich, *J. Am. Chem. Soc.*, **100**, 7094 (1978).

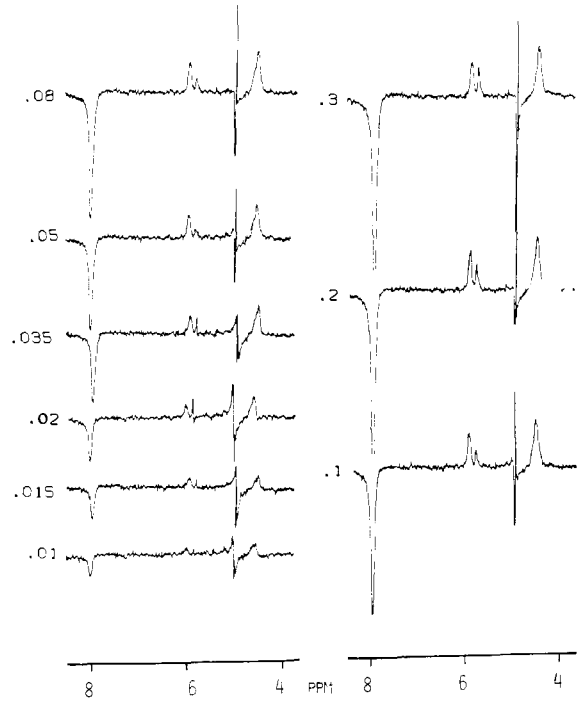

Figure 4. Difference spectra of poly(C) (70mer) following selective inversion of the H_6 resonance. Spectra were obtained at 220 MHz and 22 °C. Delay time (s) following the initial inversion pulse is indicated at the left of each spectrum.

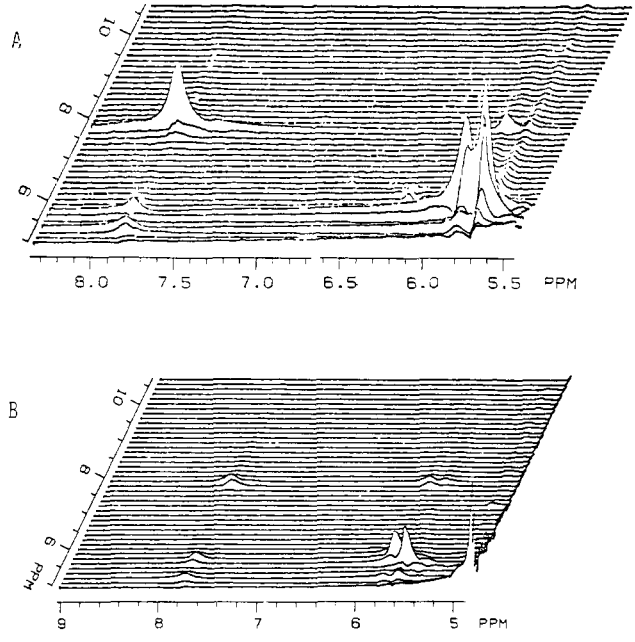

Figure 5. 300-MHz 23 °C 2D FT exchange spectrum of 95mer poly(C): (A) mixing time is 50 ms; (B) mixing time is 200 ms.

where ω_1 is the frequency of a spin during the evolution period and ω_2 is the frequency of the spin subsequent to the mixing period. The amplitudes of the cross-peaks are dependent upon τ_M, upon the exchange rates (cross-relaxation rates), and upon the direct relaxation rates; these rates are dependent upon the relevant correlation times. Because there is no chemical exchange in the poly(C) system (in D_2O), cross-peaks in the 2D spectrum will be present if there is significant spin exchange, i.e., if there are dipolar cross-relaxations among the protons in the polymer. Scalar couplings can also contribute to cross-peaks, particularly for short τ_M.[28]

Figure 5A shows the 23 °C 2D FT exchange spectrum taken with τ_M = 50 ms. The H_6, H_5, and $H_{1'}$ peaks (i.e., the normal

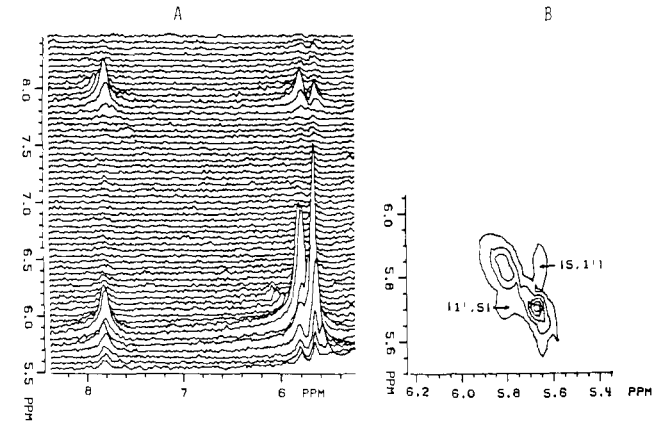

Figure 6. (A) 300-MHz 23 °C 2D FT spin exchange spectrum of 70mer poly(C); τ mixing is 250 ms; H_6–H_5, H_6–$H_{1'}$, H_5–H_6, $H_{1'}$–H_6, $H_{1'}$–H_5 cross-peaks and the H_6, H_5, $H_{1'}$ axial peaks are shown. (B) Contour plot showing the H_5 and $H_{1'}$ axial peaks and the H_5–$H_{1'}$, $H_{1'}$–H_5 cross-peaks.

one-dimensional spectrum) are along the diagonal (upper left to lower right), and the $H_6 \rightarrow H_5$, $H_6 \rightarrow H_{1'}$, $H_5 \rightarrow H_6$, $H_{1'} \rightarrow H_6$, and $H_{1'} \rightarrow H_5$ cross-peaks are clearly visible. The presence of cross-peaks in this two-dimensional spin-exchange experiment confirms the dipolar connectivities indicated by the one-dimensional experimental results. When the same experiment is run at 27 °C, the above-mentioned interactions are all present but with reduced relative intensity, as is expected. The effect of mixing time on the relative intensities of diagonal peaks to cross-peak intensities is clearly illustrated by comparing Figure 5A with Figure 5B, in which τ_M = 200 ms.

Analogous data obtained with 70mer poly(C) are shown in Figure 6. The spin interactions between the three lower field resonances are very distinct in Figure 6A, and both $H_5 \rightarrow H_{1'}$ and $H_{1'} \rightarrow H_5$ connectivities are very evident in the contour plot, Figure 6B.

Discussion

The experimental data presented in the preceding section led immediately to three conclusions. (1) The large, negative NOE's and the fact that R^0(s) is greater than R^0(ns) necessitate the existence of at least one correlation time relevant to determining ^1H relaxation rates in poly(C) that is longer than 10^{-9} s.[43] (2) The large, negative NOE's and the large number of cross-peaks in the 2D FT spectra indicate the presence of significant intramolecular dipolar interactions in poly(C). (3) Comparison of the relevant selective and semiselective rates and the appearance of the appropriate cross-peaks in the 2D FT spectra indicate there is a direct dipolar interaction between the proton at the 5-position of the cytosine ring and the proton at the 1'-position of the sugar ring that contributes significantly to the selective relaxation rates of these two protons.[43,44] Without carrying out detailed analysis, we therefore conclude that poly(C) exists for some fraction of time in an ordered structure, with relatively slow (on the nanosecond time scale) motions, in which there is an unusually short internuclear separation between the sugar $H_{1'}$ proton and the H_5 proton of the cytidine base. Since the cross-peaks in the 2D FT spectra for the H_6–H_5 and the H_5–$H_{1'}$ interactions are of comparable magnitude, we would conclude that the H_5–$H_{1'}$ internuclear distance is comparable with or shorter than the H_5–H_6 separation of 2.34 Å, since scalar coupling probably contributes some of the intensity to the H5–H6 cross-peak.

To analyze the experimental results, we briefly summarize the basic equations governing dipolar relaxation in a many-spin system. These results are then used along with the experimental relaxation data to evaluate the cross-relaxation rates, σ_{ij}, which contain the information about dipolar interactions between two spins i and

(43) J. H. Noggle and R. E. Schirmer, "The Nuclear Overhauser Effect: Chemical Applications", Academic Press, New York, 1971.
(44) N. Niccolai and E. Tiezzi, *J. Phys. Chem.*, **83**, 3249 (1979).

j. The results of the 2D spin-exchange experiments and the NOE are briefly discussed. We then consider various theoretical models for the structure and dynamics of poly(C) that might be used to account for the experimentally determined relaxation rates. Finally, we propose a three-dimensional structure for poly(C) that enables us to account for all of the important interproton interactions detected in relaxation experiments and also accounts for the unusual stability of the amino and the 2′-OH protons with respect to exchange with water previously noted by Bolton and Kearns.[37]

Review of Theory. Following a perturbation, the rate of return of the *z* component of the magnetization I_{zi} of the *i*th spin toward its equilibrium value I_{0i} can be written in the generalized form as[43-45]

$$\frac{dI_{zi}}{dt} = -\sum_j \rho_{ij}(I_{zi} - I_{0i}) - \sum_j \sigma_{ij}(I_{zj} - I_{0j}) \quad (1)$$

For a spin $^1/_2$ system undergoing isotropic rotational motion characterized by a rotational correlation time τ_c, the expressions for the direct relaxation rates (ρ_{ij}) and the cross-relaxation rates (σ_{ij}) arising from a dipolar interaction between the two spins *i* and *j* are as follows:

$$\rho_{ij} = \frac{\gamma^4\hbar^2}{10r_{ij}^6}\left[\tau_c + \frac{3\tau_c}{1+\omega_0^2\tau_c^2} + \frac{6\tau_c}{1+4\omega_0^2\tau_c^2}\right] = 2W_1^{ij} + W_2^{ij} + W_0^{ij} \quad (2)$$

$$\rho_{ij} + \sigma_{ij} = \frac{\gamma^4\hbar^2}{10r_{ij}^6}\left[\frac{3\tau_c}{1+\omega_0^2\tau_c^2} + \frac{12\tau_c}{1+4\omega_0^2\tau_c^2}\right] = 2W_2^{ij} + 2W_2^{ij} \quad (3)$$

$$\sigma_{ij} = \frac{\gamma^4\hbar^2}{10r_{ij}^6}\left[\frac{6\tau_c}{1+4\omega_0^2\tau_c^2} - \tau_c\right] = W_2^{ij} - W_0^{ij} \quad (4)$$

where γ is the nuclear gyromagnetic ratio, ω_0 is the Larmor frequency, τ_c is the rotational correlation time, r_{ij} is the internuclear separation, $\hbar$ is Planck's constant divided by 2π, and the W_k's ($k = 0, 1, 2$) are the rates (transition probabilities) of the 0, 1, 2 quantum transitions, respectively. A simple isotropic rotor model is clearly inadequate to describe the molecular motion of a partially structured molecule in solution; nevertheless, it provides a useful framework for examining the experimental results, and in a later section we discuss a theoretical model that is capable of adequately accounting for the experimental results.

The relaxation rates measured experimentally depend upon the way in which the spin system is initially prepared. If all spins in the system are initially inverted (i.e., $I_{zi} = I_{zj} = -I_{0i}$) by application of a nonselective 180° pulse, then the initial rate of return of the *i*th spin to equilibrium is, from eq 1:

$$R^0_i(\text{ns}) = \sum_{i\neq j}\rho_{ij} + \sum_{i\neq j}\sigma_{ij} \quad (5)$$

If, however, a selective 180° is applied only to spin *i* ($I_{zi} = -I_{0i}$ and $I_{zj} = I_{0j}$, initially), the initial relaxation rate is as follows:

$$R^0_i(\text{s}) = \sum_{i\neq j}\rho_{ij} \quad (6)$$

Finally, if two spins, *i* and *j*, are selectively inverted ($I_i = -I_{0i}$, $I_j = -I_{0j}$, $I_k = I_{0k}$, initially), the semiselective rates $R^0_{i,j}(\text{ss})$ for spins *i* and *j* are as follows:

$$R^0_i(\text{ss}) = \sum_{i\neq j}\rho_{ij} + \sigma_{ij} \quad (7)$$

$$R^0_j(\text{ss}) = \sum_{j\neq i}\rho_{ij} + \sigma_{ij} \quad (8)$$

Analysis of Relaxation Data. With appropriate combinations of the experimental values for the selective, nonselective, and semiselective relaxation rates, the pairwise dipolar interaction cross-relaxation rates, σ_{ij}, can be determined. Consider the semiselective and selective relaxation rates of H_5 and $H_{1'}$ at 220 MHz, 22 °C:

$$R^0_5(\text{s}) = \sum_{5\neq j}\rho_{5j} \quad (9)$$

$$R^0_{1'}(\text{s}) = \sum_{1'\neq j}\rho_{1'j} \quad (10)$$

$$R^0_5(\text{ss}) = \sum_{5\neq j}\rho_{5j} + \sigma_{51'} \quad (11)$$

$$R^0_{1'}(\text{ss}) = \sum_{1'\neq j}\rho_{1'j} + \sigma_{51'} \quad (12)$$

$$R^0_5(\text{ss}) - R^0_5(\text{s}) = \sigma_{51'} = 2.32 \pm 0.12 - 3.31 \pm 0.19 = -0.99 \pm 0.22 \quad (13)$$

$$R^0_{1'}(\text{ss}) - R^0_{1'}(\text{s}) = \sigma_{51'} = 2.96 \pm 0.17 - 3.80 \pm 0.12 = -0.84 \pm 0.21 \quad (14)$$

The average experimentally determined value of $\sigma_{51'}$ is -0.91 ± 0.22 s^{-1}.

To continue with the determination of those H_5 interactions that contribute to the spin–lattice relaxation, we note that the difference spectra resulting from the selective inversion of H_5 indicate spin transfer at similar rates to $H_{1'}$, H_6, and H_{sugar}. Any reasonable model of poly(C) that can be built suggests that $H_{2'}$ is the only upfield sugar proton that can interact directly with H_5. With this in mind, we find the following:

$$R^0_5(\text{ns}) = \sum_{5\neq j}\rho_{5j} + \sum_{5\neq j}\sigma_{5j} = 0.83 \pm 0.03 \text{ s}^{-1} \quad (15)$$

$$R^0_5(\text{s}) = \sum_{5\neq j}\rho_{5j} = 3.31 \pm 0.19 \text{ s}^{-1} \quad (16)$$

If the relaxation data determined under conditions of continuous irradiation of H_6 were accurate, this analysis would proceed smoothly.

$$R^0_5(\text{irrad H}_6) = \sum_{5\neq j}\rho_{5j} + \sum_{5\neq j}\sigma_{5j} - \sigma_{65} = \sum_{5\neq j}\rho_{5j} + \sigma_{51'} + \sigma_{52'} = 1.54 \pm 0.22 \text{ s}^{-1} \quad (17)$$

Therefore,

$$R^0_5(\text{ns}) - R^0_5(\text{irrad H}_6) = \sigma_{65} = -0.71 \pm 0.22 \text{ s}^{-1} \quad (18)$$

$$R^0_5(\text{ns}) - R^0_5(\text{s}) = \sum_{5\neq j}\sigma_{5j} = -2.48 \pm 0.19 \text{ s}^{-1} = -0.87 \pm 0.32 - 0.71 \pm 0.22 - \sigma_{52'} \quad (19)$$

$$\sigma_{52'} = -0.90 \pm 0.40 \text{ s}^{-1} \quad (20)$$

Unfortunately, $\sigma_{51'}$ is the only cross-relaxation rate in the system that could be measured directly without involving the very inaccurate measurements obtained by continuous irradiation of a given resonance. Nevertheless, if these admittedly inaccurate rates are used, manipulations of the experimental data similar to those performed above lead to a set of internally consistent cross-relaxation rates listed in Table VI. Whereas the cross-relaxations of the other protons have all been accounted for, as shown in Table

Table VI. Experimental Cross-Relaxation Rates of 70mer Poly(cytidylic acid) (220 MHz, 22 °C)

interaction	cross-relaxation rate, s^{-1}
σ_{65}	−0.71 ± 0.22
$\sigma_{62'}$	−0.86 ± 0.20
$\sigma_{61'}$	−0.88 ± 0.30
$\sigma_{52'}$	−0.90 ± 0.40
$\sigma_{51'}$	−0.91 ± 0.22
$\Sigma\sigma_{2'}$-sugars (including $H_{1'}$)	−1.24 ± 0.30
$\Sigma\sigma_{1'}$-sugars	−1.34 ± 0.30

(45) L. D. Hall and H. D. W. Hill, *J. Am. Chem. Soc.*, **98**, 1269 (1976).

Table VII. Comparison of $\Sigma\sigma$ Observed with $\Sigma\sigma$ Calculated

proton	exptl $\Sigma\sigma$,[a] s^{-1}	calcd $\Sigma\sigma$, s^{-1}
H_6	−7.23 ± 0.37	−2.45 ± 0.48
H_5	−2.48 ± 0.19	−2.48 ± 0.50
$H_{1'}$	−3.09 ± 0.13	−3.09 ± 0.38
$H_{2'}$[b]	−3.07 ± 0.16	−3.10 ± 0.55

[a] $R^0_i(\text{ns}) - R^0_i(\text{s})$. [b] If $R^0(\text{s})$ for $H_{2'} = R^0(\text{s})$ for the bulk peak H_{Sugar}.

VII, the experimental sum of the cross-relaxation rates of H_6 is much larger than the sum of its interactions with H_5, $H_{1'}$, and $H_{2'}$. Evidently H_6 interacts strongly with several of the other sugar protons, and if the rates are similar to those in Table VI, this would account for the rapid selective relaxation of H_6.

Analysis of the 2D Spin-Exchange Experiments. The 2D spectra resulting from the 2D spin-exchange experiments are shown in Figures 5 and 6. The peaks along the diagonal correspond to the regular one-dimensional spectrum, but off-diagonal peaks arise from cross-relaxation between spins i and j. For a homonuclear, two-spin system in which both spins have equal external relaxation (i.e., $\rho_{ij} = \rho_{ji} = \rho$) and all relaxation is due to intramolecular dipolar interactions, the intensities of the peaks in the 2D exchange experiment are

$$a_{ii}(\tau_M) = a_{jj}(\tau_M) = \frac{M_\infty}{4}\exp[-(\rho - \sigma)\tau_M](1 + \exp[-2|\sigma|\tau_M])$$

$$a_{ij}(\tau_M) = a_{ji}(\tau_M) = \frac{M_\infty}{4}\frac{\sigma}{|\sigma|}\exp[-(\rho - \sigma)\tau_M](1 - \exp[-2|\sigma|\tau_M]) \quad (21)$$

where $\sigma = \sigma_{ij} = \sigma_{ji}$, the a_{ii}'s are the intensities of peaks along the diagonal axis of a 2D plot, and the a_{ij}'s are the intensities of the cross-peaks.[25,27] Examination of eq 21 shows that the amplitude of the cross-peak is positive, relative to that of the axial peak, if $\sigma < 0$ and negative if $\sigma > 0$. Again, $\sigma < 0$ is indicative of long correlation times in which W_0 processes dominate.

The equations for peak intensity given above are appropriate only for a single two-spin interaction. Also, application of these equations requires knowledge of the cross-relaxation rates at 300 MHz, whereas they have been determined experimentally only at 220 MHz. Nevertheless, with the modified Woessner theory[46] discussed below to obtain $\sigma_{51'}$ at 300 MHz, the predicted ratio of the diagonal peak intensity to the cross-peak intensity in Figure 6A is 9:1 and the contour plot in Figure 6B indicates a ratio of 6:1. Given the inappropriateness of the equations used, the agreement is satisfactory.

NOE. The expression for the nuclear Overhauser effect factor, η, in a two-spin system undergoing isotropic rotational diffusion with a correlation time τ_c is[43] as follows:

$$\eta = \frac{\sigma_{AB}}{\rho} = \frac{W_2 - W_0}{2W_1 + W_0 + W_2} = \frac{\dfrac{6\tau_c}{1 + 4\omega_0^2\tau_c^2} - \tau_c}{\dfrac{3\tau_c}{1 + \omega_0^2\tau_c^2} + \tau_c + \dfrac{6\tau_c}{1 + 4\omega_0^2\tau_c^2}} \quad (22)$$

The observation that the Overhauser effect is negative at 220 MHz requires that $W_0 > W_2$, and therefore, $\tau_c > 1.1 \times 10^{-9}$. As τ_c increases beyond 10^{-9} s, the zero-quantum transition becomes the dominant spin–lattice relaxation mechanism. For example, if $\tau_c = 5.0 \times 10^{-9}$, $W_1 \sim 6\%\ W_0$, $W_2 \sim 3\%\ W_0$. In this situation the spins exchange energy among themselves much more rapidly than with the lattice, and hence cross-peaks of reasonable magnitude in the 2D exchange spectrum are expected and observed.

Possible Models of Internal Motion To Account for Observed Rates. A variety of different theoretical models for the static and dynamic behavior of poly(C) were considered in an attempt to account for the observed relaxation data, and a detailed description of that work is presented elsewhere.[47] We soon found that it was not possible to account for the observed relaxation rates with a rigid-rotor model in which all interproton distances are fixed. However, if the molecule is modeled as an anisotropically tumbling cylinder with internal motions (i.e., rotation of the interproton vectors about a rotation axis, which is inclined at some angle α relative to the cylinder axis), then it is possible by using a modified Woessner theory[46] to account for the experimentally measured relaxation rates and their frequency dependence. Some features of the model are shown in Figure 7, and the following parameters need to be defined: τ_R = correlation for end-over-end tumbling of the cylinder; τ_G = correlation time for spinning about the cylinder axis (provided $\tau_G \ll \tau_R$); τ_{int} = correlation time associated with internal motions of protons i and j; α = angle between the cylinder axis and the axis of internal rotation; Δ = angle between the interproton vector and the internal rotation axis; and $\phi''(t)$ = time dependent angle of restricted rotation of the internuclear vector about the rotation axis z', the internuclear vector being inclined at an angle between Δ and $\Delta + \delta\Delta$ relative to z'.

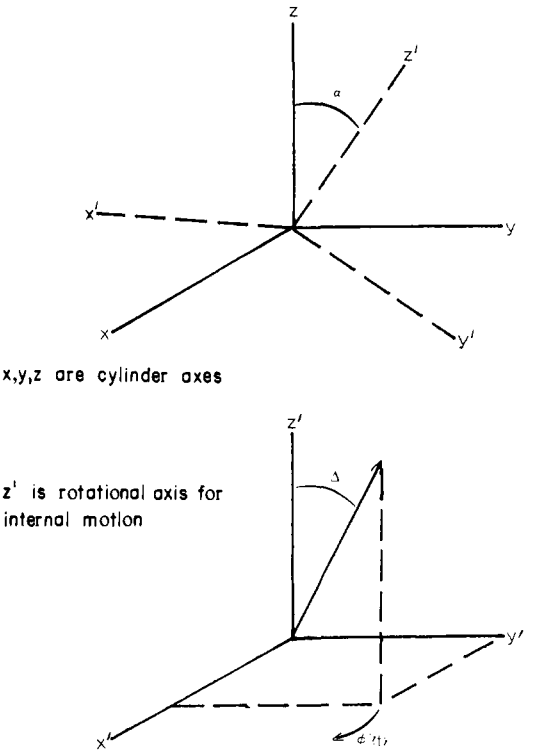

Figure 7. Coordinate system used to describe the overall and internal motions in poly(C). Z is the axis of the helix and Z' is the rotational axis for internal motion. Internuclear vector, r_{ij}, is inclined at some angle Δ relative to Z'.

The significance of $\phi''(t)$ is clarified by the following illustration. Let proton j be at some fixed position and further let r_{ij}^0 be the minimum allowed interproton separation between protons i and j. Now let proton i move a distance $\pm\Delta r_i \leq |\Delta r_i^{\max}|$ along the surface of the cone at constant latitude such that

$$r_{ij}(t) = ((r_{ij}^0)^2 + \Delta r_i^2)^{1/2} \quad (23)$$

At $\Delta r_i = 0$, $\phi''(t) = 0$, and at $\Delta r_i = \Delta r_i^{\max}$, $\phi(t) = \phi^{\max}(t)$ where

$$\phi^{\max}(t) = \sin^{-1}\frac{\Delta r_i^{\max}}{r_{ij}^{\max}} \quad (24)$$

In this way fluctuations in r_{ij} define the excursions in $\phi''(t)$. We reasonably assume that $\phi''(t)$ can be taken to have a Lorentzian

(46) D. E. Woessner, *J. Chem. Phys.*, **37**, 647 (1962).

(47) M. S. Broido, Ph.D. Dissertation, University of California-San Diego, 1980.

Table VIII. Calculated Relaxation Parameters for Poly(C)[a]

interaction H_i–H_j	τ_{int}, s	r_{ij}, Å	α, deg	Δ, deg	$\frac{\sigma^{max}}{4}$, deg	R^0_{ij} (s), 220 MHz s^{-1}	R^0_{ij} (ns), 220 MHz s^{-1}	σ_{ij}, 220 MHz s^{-1}	R^0_{ij} (ns), 300 MHz s^{-1}
6-5	5.7×10^{-9}	2.34	85	10	10	1.11	0.37	−0.74	0.24
6-1′	1.2×10^{-9}	2.39	25	25	25	1.09	0.24	−0.85	0.15
6-2′	3.9×10^{-10}	2.36	0	25	15	1.95	0.24	−1.71	0.18
6-3′	1.89×10^{-10}	2.44	15	15	24	1.83	0.10	−1.73	0.07
6-5′	9.5×10^{-10}	2.37	15	10	5	2.45	0.09	−2.35	0.05
5-1′	1.2×10^{-9}	2.49	12	29	24	1.07	0.20	−0.87	0.12
5-2′	1.5×10^{-9}	2.42	5	33	19	1.11	0.25	−0.86	0.15
1-2′	1.5×10^{-9}	3.01	0	30	4	0.36	0.06	−0.30	0.04
1′-5′ (or 3′)	3.1×10^{-10}	2.38	20	25	15	1.31	0.23	−1.09	0.18

[a] Values obtained by using $\tau_R = 2 \times 10^{-8}$ s and $\tau_G = 0.5 \times 10^{-9}$ s.

Table IX. Comparison of Calculated and Experimental Relaxation Rates for Poly(C)

	R^0(s)[a]		R^0(ns)		R^0(ns)	
proton	220 MHz exptl	calcd	220 MHz exptl	calcd	300 MHz exptl	calcd
H_6	8.28 ± 0.40	8.43	1.05 ± 0.05	1.04	0.65 ± 0.05	0.69
H_5	3.31 ± 0.19	3.30	0.83 ± 0.04	0.84	0.54 ± 0.04	0.51
$H_{1'}$	3.80 ± 0.19	3.38	0.71 ± 0.05	0.79	0.48 ± 0.04	0.48

[a] All rates s^{-1} for 70mer at 23 °C.

distribution $\rho(\phi)$ centered about $\phi''(t) = 0$. If we further define the value of $\phi^{max}(t)$ to be such that there is an 85% probability that $\phi(t) \leq \phi^{max}(t)$, then the half-width at half-height of $\rho(\phi)$ is just $\phi^{max}(t)/4$ and

$$\rho(\phi) = \frac{\phi^{max}/4}{\pi(\phi^{max}/4)^2 + \phi^2} \tag{25}$$

Clearly, with such a distribution function, r_{ij}^{max} and $\phi(t)$ are misnomers, since r_{ij} and ϕ can extend beyond their respective "maximum" values. Nevertheless, it is physically reasonable in that small amplitude fluctuations in the interproton distance are highly probable, whereas large amplitude fluctuations have a much smaller probability.

A correlation time associated with these functions must now be defined. If we assume

$$\langle \cos \phi(t) \rangle = e^{-t/\tau_i} \tag{26}$$

then from eq 25 and 26, we find

$$\langle \cos 2\phi(t) \rangle = e^{-2t/\tau_i} \tag{27}$$

and

$$\frac{\phi^{max}(t)}{4} = t/\tau_i \tag{28}$$

i.e., the maximum angular displacement that may occur in time t is dependent upon the rate of the displacement. When the above model is applied with Woessner theory[46] to poly(C), a set of parameters can be found which permit all of the experimental relaxation rates to be fit; these results are shown in Table VIII, and the resulting rates are compared with the experimental rates in Table IX. Since τ_R is expected to decrease with increasing temperature, we predict that the selective relaxation rates will decrease with increasing temperature, as observed (see Tables IV, V), and that there will be some increase in the nonselective relaxation rates as the temperature is increased (see Figure 3).

The main purpose of the above discussion is to indicate that it is possible to develop a plausible theoretical model that can account for most of the observed relaxation rates. In particular, we note that all of the relaxation rates can be accounted for by using a single value of about 12 ns for τ_R at 23 °C for the 70mer. We further note that the correlation time for internal motion, τ_{int}, is on the order of 10^{-9} s for most of the interproton interactions, although we obtain the best fit of the experimental data by using a somewhat shorter time for the interaction of H_6 with a couple of the sugar protons. We do not propose that these correlation times be taken as especially accurate. Rather, they should be viewed as better than order of magnitude values, and they are certainly reasonable in view of other studies[10,13,14] which indicate there are internal motions even in more ordered molecules, such as DNA, with time constants on the order of 1 ns. Temperature jump studies of Freier et al.[32] indicate that the lifetime of the ordered state of poly(C) is on the order of 100 ns at 23 °C, perfectly consistent with our results, which require an overall effective tumbling time of 12 ns.

While the correlation times for internal motion may be uncertain, it is not possible to account for the experimental relaxation rates without using some rather short interproton distances. Specifically, those interactions of considerable importance in the present study involve the $H_{1'}$ sugar proton and the H_5 and H_6 protons of the base. In the calculations, we find a good fit of the relaxation data by using values around 2.5 Å. Much shorter values would be totally unexpected, but if we used values much larger than 2.9 Å, it would be virtually impossible to account for the observed $H_{1'}$–H_5 cross-relaxation rate. Note also that in the calculations we assumed that the molecule spends 100% of its time in an ordered state. If, as is more likely, there is rapid equilibration between the structured state and some disordered state, then an even shorter $H_{1'}$–H_5 distance would be required. We therefore conclude that in the ordered state of poly(C) the $H_{1'}$–H_5 and $H_{1'}$–H_6 distances are quite short.

Development of a Molecular Model of Poly(C). For development of a suitable molecular structure for poly(C), models of A- and B-form polynucleotides were examined to see if the interproton distances determined for poly(C) were consistent with the common polynucleotide conformations. In neither of these two helical forms was the H_5–$H_{1'}$ distance smaller than 3.5 Å, although it became evident that the shortest H_5–$H_{1'}$ distance is between H_5 of one unit and the $H_{1'}$ proton of a neighboring mononucleotide, rather than H_5 and $H_{1'}$ protons within the same mononucleotide unit.

A Kendrew wire model corresponding to the coordinates proposed by Arnott[48] for neutral poly(C) was then built, and this, too, was found to lack the requisite short H_5–$H_{1'}$ interaction. We then searched for alterations in the Arnott structure that would bring the $H_{1'}$ proton into close proximity with the H_5 and H_6 protons with a minimum number of changes in the helical parameters without generating any repulsive atom–atom interactions. We soon discovered that changes in the backbone torsional angles lead to the requisite distances; however, these changes also converted the helix from a right-handed to a *left*-handed helix. All

(48) S. Arnott, R. Chandrasekaran, and A. G. W. Leslie, *J. Mol. Biol.*, **106**, 735 (1976).

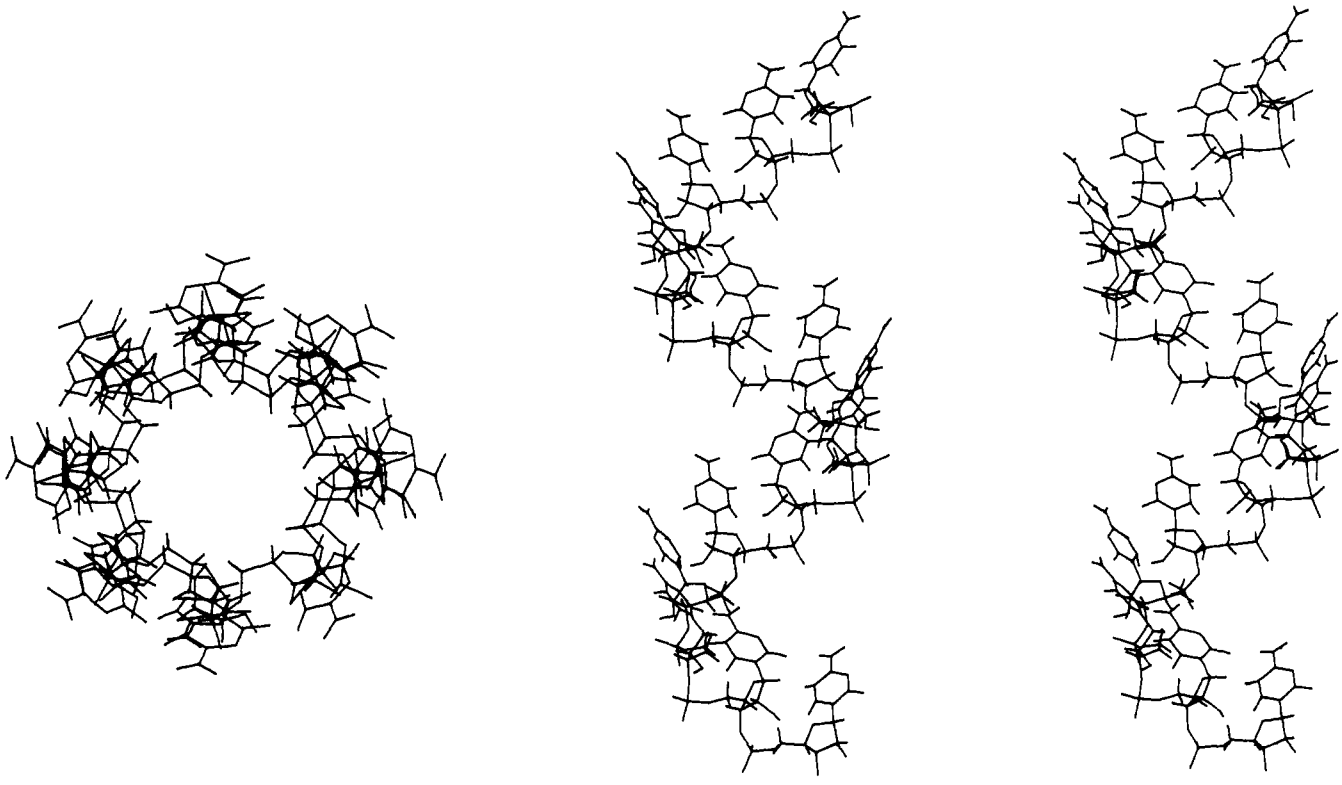

Figure 8. Stereoscopic drawing of a left-handed poly(C) helix (right). A view down the helix axis is shown on the left.

of our attempts to generate a short $H_{1'}$–H_5 interaction with a right-handed helical structure were unsuccessful. Once a reasonable structure containing the suitable interactions was found, the approximate coordinates (backbone torsion angles) were used in a computer search to generate the structure shown in Figure 8. The computer search, which was carried out by Richard Everett and Dr. Pnina Dauber, is described in the supplementary material for this paper, which also provides more specific structural details. The proposed structure has a more or less normal conformation for the sugar and regular distances for all covalently bonded atoms[48,49] and contains the requisite short distances between $H_{1'}$ and both H_5 and H_6 without generating repulsive interactions between other atoms in the molecule. The helix has a turn angle per residue of 44 ± 1° and a rise per base of 2.9 ± 0.05 Å.

Having generated a rather unexpected structure for the ordered form of poly(C), it was of interest to examine it for features that might be responsible for stabilizing it. Two unusual features were immediately evident. First, the distance between the carbonyl group of one cytosine and the amino group of an adjacent residue is ~3.0 Å and properly aligned for an amino–carbonyl hydrogen bond (see Figure 9). Second, the 2′-OH–phosphate oxygen distance is only ~2.6 Å, and this permits a direct hydrogen bond between these two groups. We further note that the bases are arranged with a very favorable head-to-tail arrangement of the dipoles. Calculations using the cytosine atomic charge distributions of Ornstein et al.[50] give a stabilization energy of about 2 kcal/mol for this arrangement. Relative to 8 kcal/mol stabilization per base pair in DNA,[2] this is not an insignificant contribution.

Comparison with Previous Studies on Poly(C). In this section we examine the proposed structure in solution in light of existing literature. Most previous studies provide little concrete information about specific structural features of poly(C). One possible exception is Fasman's study of the reaction of poly(C) with formaldehyde and his conclusion that amino hydrogen bonds are not

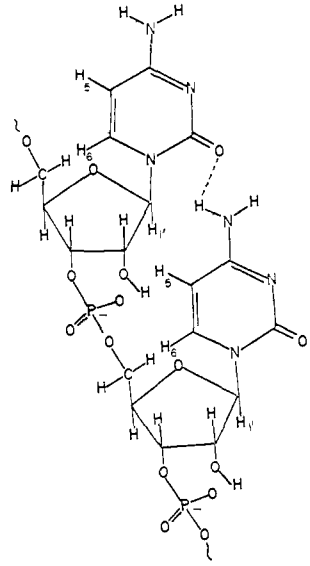

Figure 9. Section of the polynucleotide chain showing the amino–carbonyl hydrogen bond.

involved in stabilizing the ordered structure of poly(C).[31] This conclusion was based on the observation that after reaction with formaldehyde there was no change in the ORD spectrum of poly(C) whereas reaction of formaldehyde with the exocyclic amino groups of nucleic acid bases denatures DNA. However, the more recent extensive studies of McGhee and von Hippel[51] on the reaction of formaldehyde with nucleic acids and nucleic acid constituents raise questions about the interpretation of the earlier study of poly(C). In particular, the equilibrium constant for the reaction of formaldehyde with single-stranded nucleic acids, k(forward)/k(reverse), is 13.0 M^{-1} at 23 °C, but the ratio of initial rates, k(forward)/k(reverse), is 0.59 M^{-1}, and it can take 7–10 days to reach equilibrium. It is unclear from the description of the experimental conditions whether true equilibrium was reached

(49) R. H. Sarma, Ed., "Nucleic Acid Geometry and Dynamics", Pergamon Press, New York, 1980.

(50) R. L. Ornstein, R. Rein, D. L. Breen, and R. D. Macelroy, *Biopolymers*, **17**, 2341 (1978).

(51) J. D. McGhee and P. H. van Hippel, *Biochemistry*, **14**, 1281 (1975).

in Fasman's study.[31] Furthermore, hydrogen bonding between bases inhibits the rate of reaction, and it is likely that this further slowed the approach to equilibrium. With the formaldehye concentrations typically used in reactions with DNA (~0.5 M) the equilibrium percentages of the various species will be 2–15% cytosine diadduct and 55–75% cytosine monoadduct. Thus, for the majority of the bases only one of the two amino protons is unavailable for hydrogen bonding. While the monoadduct of the reaction with formaldehyde disrupts hydrogen bonds in normal Watson–Crick base pairs, this would not necessarily disrupt the hydrogen bonding in the proposed poly(C) structure. In fact, it has been shown that the monoadduct of adenine still forms a hydrogen bond with thymine, although the resultant base pair is significantly less stable than that formed with unreacted adenine.[51] We therefore conclude that the formaldehyde experiments do not rule out the proposed hydrogen bond between the amino and carbonyl groups of adjacent cytosine residues.

In support of the proposed hydrogen bonds involving the amino protons, we note that previous NMR studies indicate that the amino protons of poly(C) are unusually stable with respect to exchange with water solvent.[37] The mononucleotides of adenine and cytosine both possess exocyclic amino groups, and at 0 °C and neutral pH, the resonances from the two amino protons in AMP appear as one 10-Hz line, whereas in CMP resonances from the two amino protons are observed as two separate peaks with line widths of 20 and 50 Hz, respectively.[52] When the temperature is raised to 10 °C, the AMP amino resonance slightly broadens to 15 Hz, but the resonances from the amino protons in CMP are over 60 Hz wide. At 20 °C the AMP amino resonance is still only 20 Hz wide; however, the CMP amino resonances are broadened substantially (~150 Hz) due to rapid exchange with the solvent.[52] In the respective homopolymers, the relative stability of the amino protons is reversed. At 23 °C the amino resonance in poly(A) is already broad, and by 47 °C, it is broadened beyond detection.[40,52] By way of contrast, the amino resonances in poly(C) are rather sharp at lower temperatures (line widths on the order of those observed for the aromatic protons), and although they have started to broaden, they are still easily seen at 49 °C.[37] The fact that the amino protons of poly(C) are less susceptible to exchange with water than are the amino protons of poly(A), whereas the reverse is true of mononucleotides, clearly requires some special hydrogen-bonding interaction in poly(C) that is absent in poly(A). An amino–carbonyl hydrogen bond is a likely candidate, and it is known that hydrogen bonding of one of the two amino protons tends to reduce the exchange rate of the other amino proton.[53]

There is also NMR evidence for some special hydrogen bonding involving the 2′-OH groups in poly(C). Ordinarily the 2′-OH resonances from mononucleosides and acyclic nucleotides cannot be observed in water because of rapid exchange with the solvent. However, in the ordered double helical RNAs and in single-stranded poly(C), the 2′-OH resonances can be observed at elevated temperatures.[37] The unusual stability of the 2′-OH resonances with respect to exchange was attributed to an indirect hydrogen-bonding interaction with the phosphate group via an intervening water molecule. However, as a consequence of the altered C_3'–O_3'–P_5'–O torsion angle in poly(C) relative to A-type RNA, a direct ribose OH–phosphate hydrogen bond is possible. (A base effect on the acidity of the 2′-OH may be in part responsible for the different behavior of poly(C) as compared with other homopolymers.) This direct hydrogen bond would also account for the fact that the single-stranded (presumably helical) structure of poly(C) is more stable than the corresponding poly(deoxyribocytidylic acid).[2]

The Raman spectra of poly(C) indicate that even at high temperatures the conformation of the poly(C) backbone is not that of A-type RNA.[35,36] Perhaps the extra stability of a direct 2′-OH–phosphate oxygen hydrogen bond, as compared with an indirect interaction via an intermediate water bridge,[37] provides a possible explanation for this observation.

Raman studies of poly(C) have been interpreted to indicate that there is substantial stacking of the bases in the ordered structure.[35,36] This was based on the fact that cytosine resonances show a "normal" hypochromicity upon thermal denaturation. The direct carbonyl-to-amino hydrogen bonding between adjacent residues could provide an alternative interaction that could account for the observed hypochromicity. Chen and Charney[33] were unable to observe electric field induced birefringence in the near-UV spectrum of poly(C), and this would be consistent with our model, which has the planes of the bases tilted at about 45° relative to the helix axis. We note, however, that Causley and Johnson[34] were successful in observing a small linear dichroism in the vacuum UV spectrum of poly(C) that was ordered by flow. Freier et al.[32] have used Raman laser temperature-jump techniques to measure the kinetics of the helix to coil transition in poly(C) and find that the rate constant is on the order of 10^7 s^{-1}. These measurements indicate that poly(C) remains in an ordered state for a time that is long compared with the effective end-over-end rotational correlation time (12 ns) required to account for the observed NMR relaxation rates.

Finally, if the poly(C) adopts a left-handed helical structure one might have expected its CD spectrum would be inverted from that observed with some of the other (presumably right-handed helical) single stranded polymers. We note, however, that theoretical studies show that both left- and right-handed helices can have CD spectra with the same sign, depending upon the precise orientation of the bases relative to the helix axis.[54] Therefore, the fact that the ORD or CD spectra can be accounted for in terms of a right-handed helical structure by no means rules out the possibility that the structure is in fact left-handed. Moreover, recent calculations of the CD spectrum of the left-handed Z-type DNA predict a spectrum in which even the signs of the peaks are in disagreement with the experimental results.[55]

Summary

In summary, our NMR proton relaxation measurements unequivocally demonstrate that in the ordered state of poly(C) there is a short separation between the $H_{1'}$ sugar proton and the H_5 and H_6 protons of the base. To account for this unexpected interaction, we propose a novel, left-handed helical structure with stabilizing hydrogen bonding interactions between the amino and carbonyl groups of adjacent bases and between the 2′-OH group and the phosphate group. This structure is consistent with most of the literature regarding the structure of poly(C) in solution, and evidence for the two important hydrogen bonding interactions already exists in the literature. The apparent discrepancy with some of the earlier evidence regarding the role of the amino hydrogen bonds has been reevaluated in light of more recent studies of the reaction of formaldehyde with polynucleotides. The most unusual aspect of the proposed structure is that it is a *left*-handed helix, and this is seen to arise from the hydrogen-bonding properties of cytosine, which allow for the formation of a hydrogen-bonding network between the amino and carbonyl groups. This study represents the first application of 2D Fourier transform NMR techniques to a polynucleotide, and we anticipate that these and related pulsed NMR methods will prove to be of significant value in the investigation of the solution state structure of other polynucleotides.

Acknowledgment. The support of the U.S. Public Health Service (Grant GM-22969 and in part RR 00757) is most gratefully acknowledged. We particularly thank Dr. D. Lerner for preparing the poly(C) samples used in these experiments, and Dr. J. Wright for technical aid, and R. Everett and Pnina Dauber

(52) M. Razka and N. O. Kaplan, *Proc. Natl. Acad. Sci. U.S.A.*, **69**, 2025 (1972).
(53) C. Mandal, N. R. Kallenbach, and S. W. Englander, *J. Mol. Biol.*, **135**, 391 (1979).
(54) E. Charney in "The Molecular Basis of Optical Activity", Wiley, New York, 1979.
(55) H. Vasmel and J. Greve, *Biopolymers*, **20**, 1329 (1981).

for preparing the computer-generated structure.

Registry No. Poly(C), 30811-80-4.

Supplementary Material Available: a description of the computer graphics system used to obtain a refined model of the poly(C) structure, tables of the backbone and base rotation torsion angles and sugar torsion angles in the proposed structure for poly(C) and cylindrical coordinates for a typical residue in poly(C), and figures that show the structure of the monomer unit of 5'-monophosphate cytidine and a stereoview of the left-handed poly(C) structure (6 pages). Ordering information is given on any current masthead page.

Autoxidation of Model Membrane Systems: Cooxidation of Polyunsaturated Lecithins with Steroids, Fatty Acids, and α-Tocopherol

Hugo Weenen and Ned. A. Porter*

Contribution from the Paul M. Gross Chemical Laboratories, Duke University, Durham, North Carolina 27706. *Received September 8, 1981*

Abstract: The autoxidation of diL-PC and 1S,2A-PC in aqueous emulsion with several cosubstrates was investigated. Cholesterol, 7-dehydrocholesterol, linoleic acid, and α-tocopherol were cosubstrates in the autoxidation of dilinoleoylphosphatidylcholine (diL-PC). The distribution of the products, *tc* and *tt* diene hydroperoxides, was determined and evaluated. It was concluded that cholesterol has a lower H atom donating ability (K_p) and 7-dehydrocholesterol a much higher K_p than diL-PC. Linoleic acid when mixed with diL-PC, diP-PC, or a mixture of the two was found to behave analogous to a mixture of just the two lecithins. The cooxidation of diL-PC with α-tocopherol in the bilayer gave only *trans,cis* (*tc*) hydroperoxides, which can be ascribed to a very high k_{inh} for α-tocopherol, a very efficient antioxidant. 1-Stearoyl-2-arachidonoylphosphatidylcholine (1S,2A-PC) bilayer autoxidation gave a product distribution very similar to arachidonic acid neat autoxidation. However the products from cooxidation of a 1S,2A-PC bilayer with α-tocopherol unexpectedly did not include the 5-hydroperoxy eicosatetraenoic acid isomer (5-HPETE), although the 12, 15, 11, 9, and 8 isomers were present in almost equal amounts.

Lipid peroxidation is an important process leading to a class of compounds that play a central role in a variety of biological events such as inflammation,[1] platelet aggregation,[2] asthma,[3] and anaphylaxis.[4] Under normal conditions, enzymatic oxidation seems to be the predominant process; however, random autoxidation of polyunsaturated fatty acids also appears to be an important process[5] in vivo as evidenced by the expiration of pentane and ethane, known fatty acid oxidation products, by organisms under free-radical stress. Membrane damage induced by radiation[6] and carbon tetrachloride or ethanol poisoning[7-9] has been proposed to be the result of phospholipid destruction by molecular oxygen. In fact, a theory of aging has been proposed that rests in part on the free-radical oxidation of membrane lipid.[10] Reincorporation of an oxidized fatty acid formed enzymatically into human neutrophil membrane phosphatidylcholines (PC) in vivo suggests a biological role for PC oxidation products.[11] Lipid oxidation, both enzymatic and nonenzymatic, is also an important factor in the oxidative deterioration of food products,[12] which has been suggested to produce carcinogens.[13] A physiological role for the plant lipoxygenase pathway has not yet been established.

In light of the potential importance of phospholipid oxidation products, we have studied the autoxidation of the polyunsaturated lecithins **1** and **2** in the presence of some natural membrane

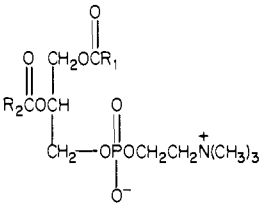

1, $R_1 = R_1$ = linoleate; diL-PC
2, R_1 = stearate, R_2 = arachidonate; 1S,2A-PC
3, $R_1 = R_2$ = palmitate; diP-PC

constituents such as steroids, fatty acids, saturated lecithin **3**, and α-tocopherol. We recently reported on the isolation and analysis of PC hydroperoxides[14] and on the factors controlling the stereochemistry of hydroperoxides produced by autoxidation of linoleic acid.[15] The proposed mechanism of *trans,cis* (*tc*) and *trans,trans* (*tt*) hydroperoxide formation is outlined in Scheme I.

Thus 13-peroxy-*trans,cis*-dienyl (13-*tc*) radical (conformers **5a** + **5b**) can lead to the 13-*tc* hydroperoxide **6** or (via conformer **5b**) can undergo β scission and eventually lead to the 9-*tt* hydroperoxide **8**. Similarly, a 9-*tc* peroxy radical can give the 9-*tc* hydroperoxide or (via conformer **5b**) can be converted to the 13-*tt* hydroperoxide. Analysis of the mechanism shown in Scheme I by using steady-state assumptions leads to eq 1, where [L-H] is

$$\frac{tc}{tt} = \frac{k_p[\text{L-H}]}{k_\beta(1-\alpha)} + \frac{\alpha}{1-\alpha} \qquad (1)$$

the concentration of linoleic acid, k_p is the rate constant for propagation, k_β is the rate constant for β fragmentation of peroxy radicals, and α and $(1-\alpha)$ refer to the partitioning of carbon radicals between the *tc* peroxy radical **5b** and the *tt* peroxy radical

(1) Kuehl, F. A. *Science (Washington, D.C)* **1980**, *210*, 978.
(2) Salomon, J. A.; Smith, D. R.; Flower, R. J.; Moncada, S.; Vane, J. R. *Biochim. Biophys. Acta* **1978**, *523*, 250.
(3) Parker, C. W. *Allergy Clin. Immunol.* **1979**, *63*, 1.
(4) Corey, E. J.; Barton, A. E.; Clark, D. A. *J. Am. Chem. Soc.* **1980**, *102*, 4278.
(5) Tappel, A. L.; Dillard, C. J. *Fed. Proc., Fed. Am. Soc. Exp. Biol.* **1981**, *40*, 174.
(6) Wills, E. D. *Int. J. Radiat. Biol Relat. Stud. Phys., Chem. Med.* **1970**, *17*, 217.
(7) Weddle, C. C.; Hornbrook, K. K.; McKay, P. B. *J. Biol. Chem.* **1976**, *251*, 2973.
(8) Recknagel, R. O. *Pharmacol. Rev.* **1967**, *19*, 145.
(9) Litov, R. E.; Irving, D. H.; Downey, J. E.; Tappel, A. L. *Lipids* **1978**, *13*, 305.
(10) Tappel, A. L. *Geriatrics* **1968**, *23*, 97.
(11) (a) Stensen, W. F.; Parker, C. W. *J. Immunol.* **1980**, *124*, 2100. (b) Stenson, W. F.; and Parker, C. W. *Prostaglandins* **1979**, *18*, 285. (c) Bonser, R. W.; Siegel, M. I.; Chung, S. M.; McConnell, R. T.; Cuatrecasas, personal communication.
(12) Sessa, D. J. *J. Agric. Food Chem.* **1979**, *27*, 2.
(13) Shamberger, R. J.; Anderone, T. L.; Willis, C. E. *J. Natl. Cancer Inst.* **1974**, *53*, 1771.
(14) Porter, N. A.; Wolf, R. A.; Weenen, H. *Lipids*, **1980**, *15*, 163.
(15) Porter, N. A.; Weber, B. A.; Weenen, H.; Khan, J. A. *J. Am. Chem. Soc.* **1980**, *102*, 5597.

0002-7863/82/1504-5216$01.25/0